Available online at www.sciencedirect.com
SCIENCE DIRECT®
Wear 259 (2005) 1482–1489
WEAR
www.elsevier.com/locate/wear

Short communication

Wear monitoring of bearing steel using electrostatic and acoustic emission techniques

Jun Sun [a,*], R.J.K. Wood [a,**], L. Wang [a], I. Care [b], H.E.G. Powrie [c]

[a] *Surface Engineering and Tribology Group, School of Engineering Sciences, University of Southampton, Room 3011, Highfield, Southampton SO17 1BJ, UK*
[b] *Rolls-Royce plc, ML-77, PO Box 31, Derby DE24 8BJ, UK*
[c] *Smiths Aerospace Electronic Systems–Southampton, School Lane, Chandlers Ford, Hampshire SO53 4YG, UK*

Received 9 September 2004; received in revised form 28 January 2005; accepted 2 February 2005
Available online 10 May 2005

Abstract

Both acoustic emission (AE) and electrostatic (ES) wear monitoring are emerging as useful real-time condition monitoring techniques. These techniques are believed to be sensitive to different aspects of the physics of contact and surface degradation prior to the onset of severe wear. Thus, if both systems are used to monitor tribo-contacts, the physics of early contact degradation could be elucidated and the potential of the systems to detect precursors to severe wear could be investigated. This paper uses AE and ES charge signals generated by a bearing steel contact under dry sliding conditions to monitor the various phases of delamination wear. Tests were undertaken using an instrumented pin-on-disc (PoD) tribometer, which enabled continuous measurement of friction, surface temperature, linear wear, AE and ES signals. The AE and ES results were found to correlate with friction levels and wear rates. From the friction level, three distinct regions were identified and the wear mechanisms within each region were found (by SEM and EDS analysis) to be running-in, delamination/oxidation and oxidation.

Keywords: Acoustic emission; Electrostatic sensing; Dry sliding; Wear monitoring; Delamination

1. Introduction

1.1. Background

On-line sensing techniques for monitoring wear, deterioration and failure in real time are desired because conventional methods that rely on post processing are of limited value in providing timely information on the dynamics of the wear processes. The combination of acoustic emission (AE) and electrostatic (ES) sensing techniques has the potential to be sensitive to different aspects of the physics of contact and surface degradation prior to the onset of severe wear, which is the motivation for the current work.

1.2. Fundamentals of acoustic emission

AE is the phenomenon of transient elastic wave generation in materials under stress. When the material is subjected to stress at a certain level, a rapid release of strain energy takes place in the form of elastic waves that can be detected by transducers. Typical AE signal frequency range is between 20 kHz and 1 MHz. When surface traction occurs at asperity contacts, materials can exhibit two basic responses: elastic and plastic deformation of the surface and subsurface and fracture, which are potential AE sources [1,2].

Fig. 1 shows a schematic of the AE system used to monitor the ball on flat contact studied in this paper.

In metal to metal sliding contacts, the possible AE sources due to friction and wear include: (i) contact surface damage [1,2], (ii) subsurface cracking, nucleation and propagation [3,4], (iii) phase changes [5,6], (iv) chemical reactions [7,8], (v) impulsive shocks due to asperity collision and debris [9]

* Corresponding author. Tel.: +44 2380598331; fax: +44 2380593016.
** Co-corresponding author.
E-mail addresses: j.sun@soton.ac.uk (J. Sun), rjw3@soton.ac.uk (R.J.K. Wood).

0043-1648/$ – see front matter © 2005 Elsevier B.V. All rights reserved.
doi:10.1016/j.wear.2005.02.021

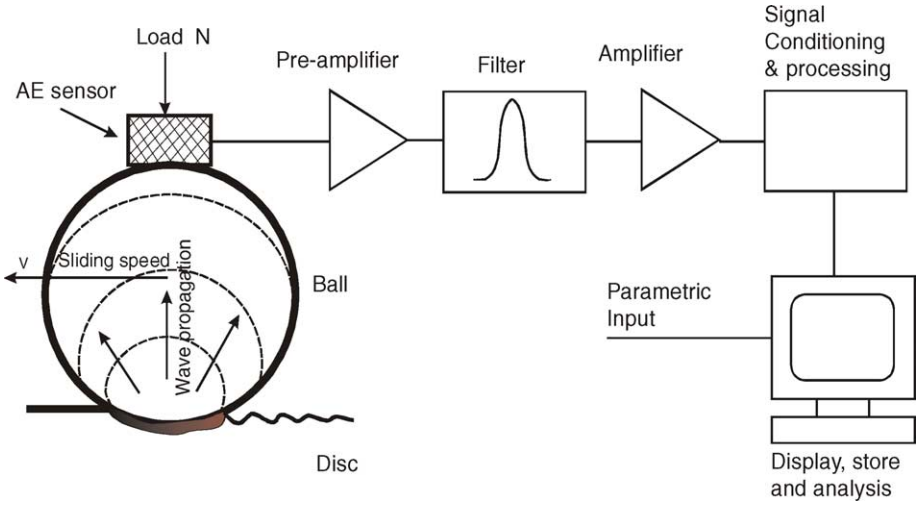

Fig. 1. Schematic of the AE monitoring system for a ball on flat sliding tribo-contact.

and (vi) micro-vibration excited by the stick-slip at the interface [10,11]. Fig. 2 illustrates the possible AE sources from a tribological contact.

Researchers have tried to find relationships between the AE parameters and different wear mechanisms. For dry sliding, various statistical AE parameters have been used in an attempt to correlate AE signals to wear trends. For example, the distribution of the number of events characterised by peak amplitude and by rise time has been investigated by McBride et al. [12]. They suggested that the actual removal of material was characterised by high amplitude, short rise time AE signals and that running-in wear and plastic flow results in lower amplitude, longer rise time signals. Jiaa and Dornfeld [13] investigated the AE signals generated from the sliding contact of metal-metal pairs on a pin-on-disc test rig and found a correlation between the AE RMS signal and the different wear mechanisms. Hanchi and Klamecki [14] showed that variations in AE count rates reflected the variations in wear rate across the mild-severe wear transition in dry sliding. Boness et al. found a strong relationship between ball wear scar volume and the integrated AE RMS signal for a dry sliding steel on steel contact [15].

1.3. Fundamentals of electrostatic sensing

Fig. 3 shows a schematic of the electrostatic charge sensing system. When a charged particle passes the electrostatic sensor face, an opposing charge will be induced on the sensor surface. The electrons in the sensor will redistribute to balance the additional charge in the vicinity of the sensor face resulting in a current flow, which can be measured.

The possible electrostatic charge sources are tribocharging [17], tribochemistry [18], contact charging [19], triboemission [20], contact potential difference (CPD) [21] and wear debris [22]. Fig. 4 shows these sources and the possible causes.

Previous work on wear monitoring has been conducted using electrostatic monitoring on Gears [23]. Specifically designed electrostatic sensors, both wear-site sensor (WSS) and oil-line sensor (OLS), have been installed to monitor actural bearings in a European project (ATOS, Brite Euram Contract G4RD-CT-2000-00391). OLSs were mounted on the oil scavenge line to monitor bearing wear debris. WSSs were successfully mounted inside the bearing chamber of full scale bearing tests facilities at General Electric, Timken and FAG.

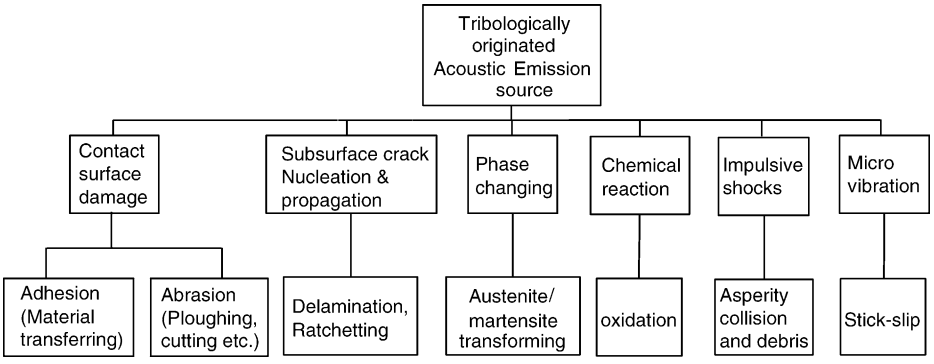

Fig. 2. Possible AE sources from a tribological contact.

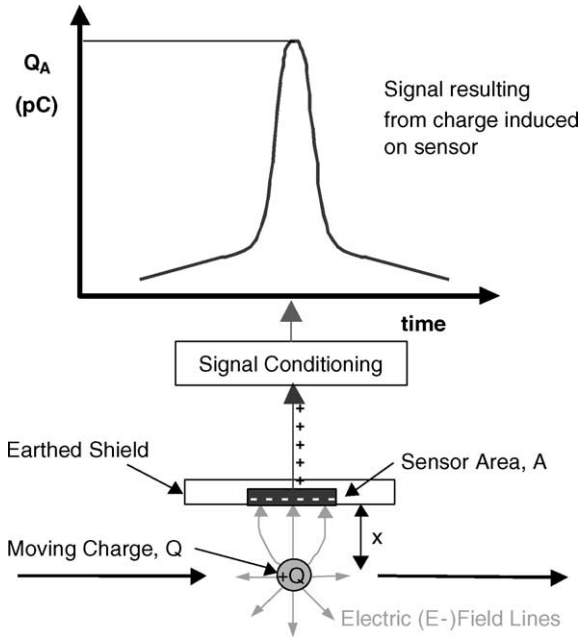

Fig. 3. Schematic of ES sensor principle [16].

2. Experimental details

2.1. Apparatus and test conditions

All tests were carried out on a modified PoD tribometer, see Fig. 5. Seven sensors were installed for on-line monitoring.

- A tachometer monitored the disc rotation speed.
- A button type electrostatic probe or WSS was located 120° downstream of the pin and disc contact point and 0.5 mm above the disc surface to monitor the charge level on the wear track.
- A strain gauge monitored the contact friction force.
- An linear-variable-differential-transformer (LVDT) monitored the vertical displacement. This enabled the linear pin and disc wear to be recorded.
- An infrared thermometer monitored the disc surface temperature (the focal point was positioned about 10 mm away from the pin and disc contact point).

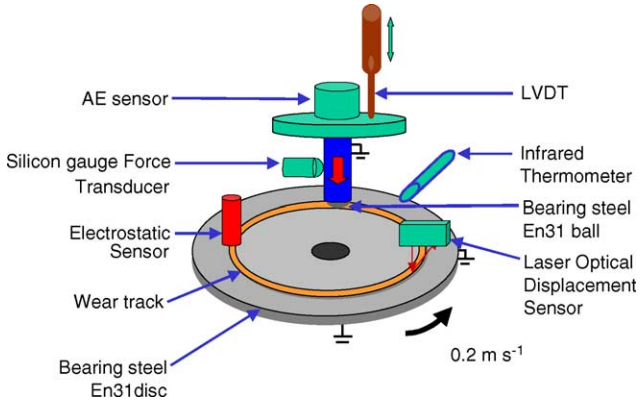

Fig. 5. Schematic of the test set-up.

Table 1
Summary of the dry sliding test conditions

	Long-distance	Specific-time-terminal
Pin/disc materials	En31/En31	En31/En31
Load (N)	5	5
Initial Hertzian contact (GPa)	1.1	1.1
Sliding velocity (m/s)	0.2	0.2
Test duration (s)	10,800	Variable
Temperature (°C)	17–23	20–21
Humidity (%)	33–59	48–53
Wear track diameter (mm)	30	30

- A laser optical displacement probe monitored the disc wear track.
- An AE wideband (WD) transducer from physical acoustic corporation (PAC) was positioned on the top of the pin holder to monitor the AE signals from the contact. The transducer had a relatively flat frequency response within 20 dB of peak sensitivity between 100 kHz and 1 MHz.

Experiments were designed to generate simple wear mechanisms from a bearing steel dry sliding contact, with the aim of correlating the wear mechanisms, identified from SEM/EDS analysis of the pin wear scar, disc wear track and debris, with the recorded ES and AE signals. The test conditions were chosen to generate a delamination wear mechanism from a dry steel sliding contact (according to the

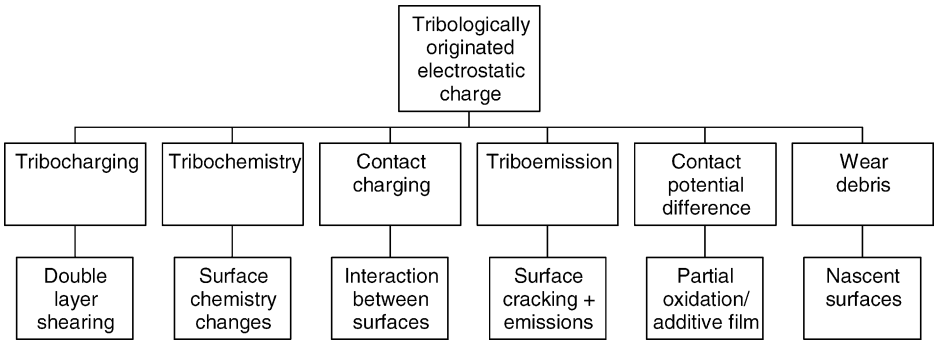

Fig. 4. Possible electrostatic charge sources in tribology.

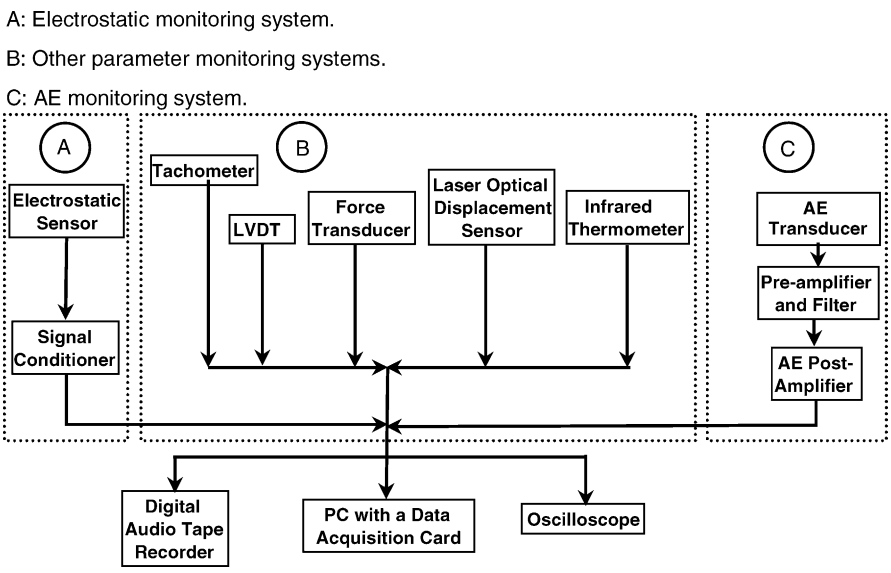

Fig. 6. Schematic of the PoD instrumentation signal acquisition and processing.

Lim-Ashby wear map [24]), which are detailed in Table 1. During the tests, the wear debris remained on the disc due to the horizontal layout of the rig.

Two types of tests were conducted in this study, i.e. a 'long-distance' test and a 'specific-time-terminal' test. The long-distance tests were run for 3 h to investigate the development of wear characteristics. Based on the information obtained from the five repeated 'long-distance' tests, which showed repeatable features on AE RMS signals, three distinctive regions were identified (see Fig. 7).

Following on from the long-distance tests, 'specific-time-terminal' tests were conducted to identify wear mechanisms within each region. For Region I, tests were stopped around 500 s after the test was started while the AE RMS trend was decreasing. For Region II, it was intended to catch a peak of a major AE feature (periodic perturbations) after 3000 s of testing. Region III was effectively the end of the 'long-distance' test when steady state conditions persist.

After each test, the wear scar of the pin, as well as the wear track of disc, were measured and the volume losses were

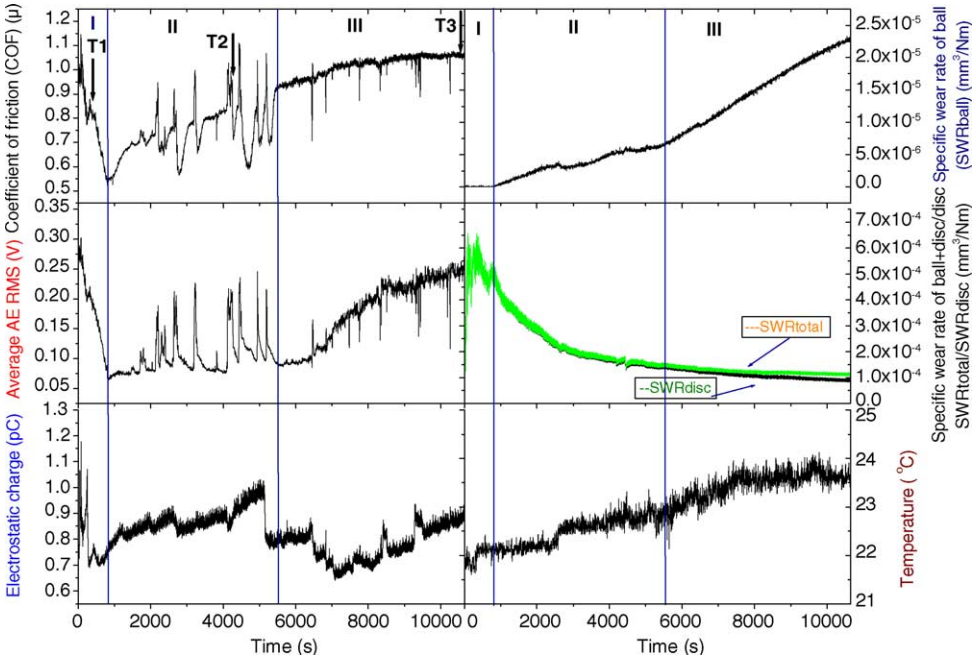

Fig. 7. The test results from the long-distance dry sliding test. N.B.: (1) SWRtotal is the sum of the specific wear rate of pin and disc, SWRpin is the specific wear rate of pin, SWRdisc is the specific wear rate of disc. (2) 'Specific-time-terminal' tests that were stopped at the times indicated by the arrows T1, T2 and T3.

calculated accordingly. The instantaneous disc and pin wear rates were also obtained from the laser optical displacement sensor and LVDT on-line measurements.

2.2. Data acquisition and signal processing

Signals from the PoD rig sensors were acquired and processed in real-time using a PC based data acquisition/processing system, which is illustrated in Fig. 6. The whole system can be split into three blocks A (ES signals), B (other PoD sensors) and C (AE signals). A Digital Audio Tape (DAT) recorder was used to record the raw data as a backup and an oscilloscope was used to show the traces of the tachometer, ES, AE and LVDT signals in real time.

Signals from all sensors were fed into a data acquisition system on a PC and were sampled at 500 Hz. Signals were then processed to give mean values (for friction, LVDT, AE RMS, temperature and laser displacement) and RMS values (for ES signals) every 4 s.

3. Results and discussion

Fig. 7 shows representative real time signals for the long-distance tests. Three distinct regions were identified (I, II and III) based on the AE features. The 'specific-time-terminal' tests were stopped at the points indicated by arrows T1, T2 and T3 and the corresponding SEM images of pin, disc and wear debris are shown in Fig. 8.

3.1. Region I

Overall, in this region the AE, ES and coefficient of friction (COF) all decrease by significant levels from their initial values at the start of the test (see Fig. 7), and the disc wear rate is relatively high while the pin wear rate was immeasurable. It should be mentioned that during the early stage of this region (the first 200 s), sudden changes on all the signals are possibly associated with material transfer from the disc to the pin.

Fig. 8a–c are the SEM images of the pin, disc and wear debris in Region I, respectively. Severe plastic deformation along with the onset of delamination wear [25,26] can be seen on the pin and disc surfaces, which generated large plate-like debris (>5 μm).

3.2. Region II

In this region, different features are found for the COF, AE and ES signals (see Fig. 7). The COF trace shows significant bipolar perturbations superimposed on an increasing background signal. The AE RMS signal has positive perturbations, which coincide with the COF, superimposed onto a constant background signal. The ES signal has an increasing background level with less obvious perturbations. During this period the disc wear rate decreases while the pin wear rate slowly increases. A modest temperature increase of 1 °C occurs. Within this region the contact area is gradually increasing resulting in decreasing contact pressure and the

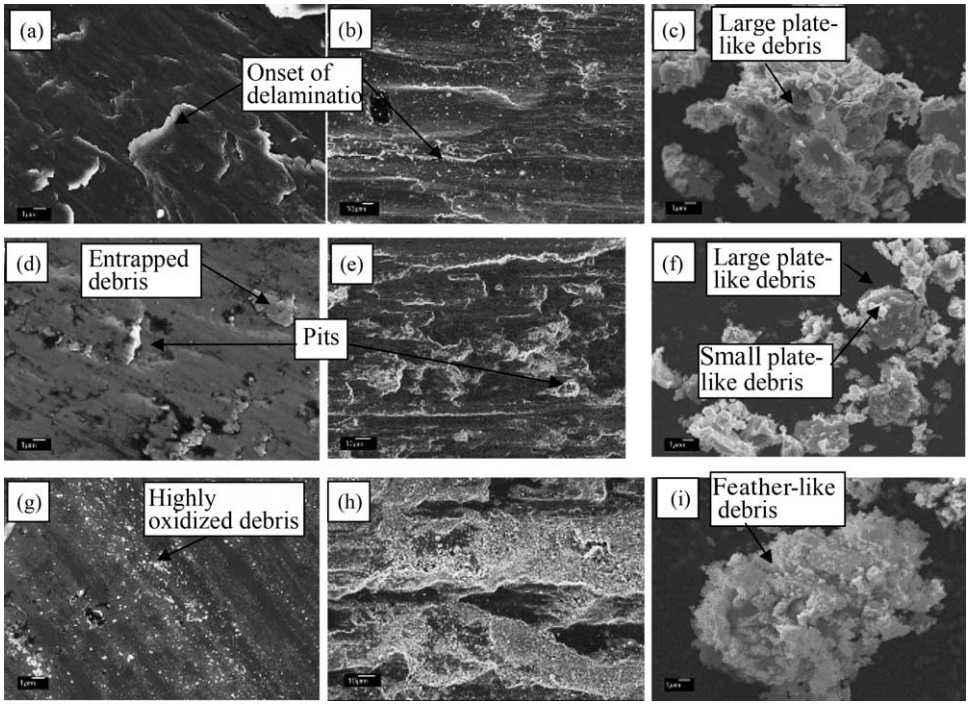

Fig. 8. Micrographs of the pin scars, disc wear track and debris for the tests stopped in Regions I, II and III, respectively, as indicated by arrows T1, T2 and T3 in Fig. 7.

Table 2
Summary of correlations between predominant wear mechanisms and sensor responses

	Region I, running-in	Region II, delamination	Region III, oxidation
Dominant wear mechanisms and debris analysis	Material transfer Onset of delamination High disc wear rate, immeasurable ball wear Large plate-like debris (>5 μm)	No material transfer Delamination Transaction between high and load wear rate Small plate-like debris (around 1 μm)	No material transfer Delamination/oxidation Low disc wear rate, high ball wear rate Fine debris (<1 μm) agglomerated feather-like debris
Sensor responses			
AE RMS	AE↓	AE↔ with +ve perturbations	AE↑ with −ve perturbations
ES Charge	ESP↓	ESP↑	ESP↑ with +ve perturbations
Friction	COF↓	COF↑ with + bipolar perturbations	COF↑ with −ve perturbations

combined pin and disc wear rate decreases from 5×10^{-4} to 1.5×10^{-4} mm^3/Nm.

SEM micrographs of the pin and disc (Fig. 8d and e) show features of delamination. Platelet ejection forms pits on the surfaces possibly induced by a ratchetting type mechanism [26]. The debris from this region is plate-like (around 1 μm) (see Fig. 8f). However, EDX analysis shows the presence of oxygen in the wear debris. This is evidence that oxidation has also been initiated at this stage of the test.

3.3. Region III

A plateau is seen between 5400 and 6300 s on the AE and ES signals and there is only a modest increase in the level of COF at the start of this region. This plateau region is followed by a small increase in COF with negative perturbations, which is mirrored by the AE response. The ES signal shows a fluctuating background level with positive, long-duration perturbations that are coincident with the friction and AE patterns. However, not all AE and COF features are seen by the ES probe. The disc wear rate slightly decreases while the pin wear rate increases significantly.

Fig. 8g and h show the micrographs of the pin and disc surfaces, which are covered by sub-micron scale debris. EDX results indicate that the debris are oxygen rich and that tribochemical wear (oxidation) is possibly the major wear mechanism in this region. The disc surface is more fragmented with larger scale delamination features and some shallow continuous grooving. This shows the sliding pair is now in a mild oxidative wear regime [27]. The wear debris (see Fig. 8i) from this region is 'feather-like' and is agglomerated fine debris (<1 μm).

Table 2 summarises the correlations between the predominant wear mechanisms and responses from the AE, ES and friction sensors in each region. Clearly the process of contact degradation is complex, involving multiple mechanisms.

In the running-in region (I), the decline in activity from a high level on the AE, ES and friction traces possibly represents the decline in asperity–asperity welding/adhesion and asperity removal. For Region II, delamination processes dominate generating a loosely adhered set of platelets on the wear surfaces. Platelet formation and then removal influences the friction (seen as oscillations), as does the unsteady debris entrainment into the contact. For Region III, the oxidation region, the perturbations in the AE, ES and COF are consistent with a transition between metal–metal contact and oxide–oxide contact initiated by oxide film growth within the contact. Oxidised debris entrained into the contact can prevent or decrease metal-to-metal contact and thereby influence friction. COF levels are also dependent on the state of iron oxides [28]. Morris et al. have shown that for dry steel on steel sliding contacts, when oxide is present, low COF values result and when no oxide is present, high values of COF occur [29]. This results in negative perturbations on the AE signal and positive perturbations on the ES, which are related to contact potential differences between oxidised and virgin surfaces. The general increases in background levels for both AE and ES may be linked to the increase in pin wear over this region.

3.4. Integrated AE RMS versus pin wear volume

Fig. 9 shows the results of integrated AE RMS vs. ball volume loss. The integrated AE RMS is calculated as

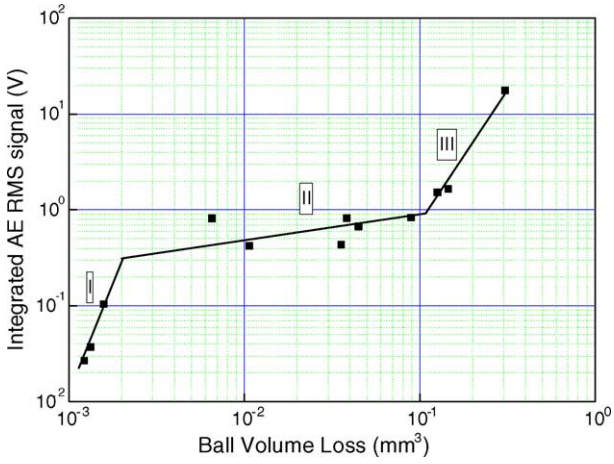

Fig. 9. Integrated AE RMS vs. ball volume loss.

below:

$$\text{Integrated RMS} = \int_0^t (\text{RMS})\,\mathrm{d}t;$$

where t is the experimental duration. RMS is the AE RMS output of the AE2A post-amplifier.

Three different linear relationships between the integrated AE RMS and pin volume loss are found for the three wear regions. In the running-in and oxidation wear regions, the AE has higher sensitivity to the ball wear compared to the delamination region. Thus, the integrated AE RMS is a promising parameter for detection and monitoring of wear in dry sliding contacts [15].

4. Conclusions

Although it is not known at this stage what the individual sensitivities of the AE and ES sensors to surface degradation are, it is encouraging that they respond differently and thus maybe detecting different aspects of contact breakdown. Some conclusions are drawn below:

- Three wear regimes were distinguished through the life of the tests as running-in, delamination and oxidation. Distinct friction, AE RMS and ES features were found for each regime which has a different dominant wear mechanism and good correlation was found between AE RMS and friction signals in all tests.
- The AE RMS and ES signals are sensitive to different aspects of contact breakdown during dry sliding wear. The combination of these two technologies may provide a more complete picture of the wear phenomena between contacting surfaces and to detect the dominant wear mechanisms within dry sliding steel contacts.
- Integrated AE RMS is highly sensitive to running-in and oxidation wear under the test conditions of this study.

Acknowledgments

This research was supported by Rolls-Royce Aerospace and Smiths Aerospace. The authors wish to thank Mr. Hill and Dr. Webster for their support and valuable suggestions. The support from the members of Surface Engineering and Tribology Group at the University of Southampton is greatly appreciated.

References

[1] N.P. Suh, Tribolophysics, Prentice-Hall, Englewood, NJ, 1986.
[2] R.V. Williams, Acoustic Emission, Adam Hilger, 1980.
[3] J.H. Williams, D.M. Delonga, S.S. Lee, Correlations of acoustic emission with fracture mechanics parameters in structural bridge steels during fatigue, Mater. Eval. 40 (11) (1982) 1184–1189.
[4] K. Sano, K. Fujimoto, Microscopic aspects of fracture and acoustic emission in metals, in: K. Ono (Ed.), Fundamentals of Acoustic Emission, University of California, Los Angeles, CA, 1979, pp. 131–164.
[5] S.M.C. van Bohemen, J. Sietsma, M.J.M. Hermans, I.M. Richardson, Kinetics of the martensitic transformation in low-alloy steel studied by means of acoustic emission, Acta Mater. 51 (14) (2003) 4183–4196.
[6] M. Landa, M. Chlada, Z. Prevorovský, V. Novák, P. Sittner, Non-destructive evaluation of phase transformations in Cu based shape memory alloys by ultrasonic techniques, in: P. Mazal (Ed.), Proceedings of International Conference “Acoustic Emission’99”, Brno, 1999, pp. 123–130.
[7] Y.P. Kim, M. Fregonese, H. Mazille, D. Féron, G. Santarini, Ability of acoustic emission technique for detection and monitoring of crevice corrosion on 304L austenitic stainless steel, NDT E Int. 36 (8) (2003) 553–562.
[8] P. Mathers, Million dollar savings: you just have to listen, Bulk Distributor 10 (5) (1998) 22.
[9] R.S. Sayles, S.Y. Poon, surface topography and rolling element vibration, Precision Eng. 3 (1981) 137–164.
[10] F.P. Bowden, L. Leben, The nature sliding and the analysis of friction, Proc. R. Soc. Lond., Ser. A, Math. Phys. Eng. Sci. 169 (1993) 371–391.
[11] D.A. Dornfeld, C. Handy, Slip detection using acoustic emission signal analysis, in: Proceedings of the IEEE International Conference on Robotics and Automation, Raleigh, NC, March 1987, New York, 1987, pp. 1865–1875.
[12] S.L. McBride, R.J. Boness, M. Sobczyk, M.R. Viner, Acoustic emission from lubricated and unlubricated rubbing surfaces, J. Acoustic Emission 8 (12) (1989) 192–197.
[13] C.L. Jiaa, D.A. Dornfeld, Experimental studies of sliding friction and wear via acoustic emission signal analysis, Wear 139 (1990) 403–424.
[14] J. Hanchi, B.E. Klamecki, Acoustic emission monitoring of the wear process, Wear 145 (1991) 1–27.
[15] R.J. Boness, S.L. McBride, M. Sobczyk, Wear studies using acoustic emission techniques, Tribology Int. 23 (5) (1990) 291–295.
[16] H.E.G. Powrie, R.J.K. Wood, T.J. Harvey, L. Wang, S. Morris, Electrostatic charge generation associated with machinery component deterioration, 2002 IEEE Aerospace Conference Proceedings, ISBN 0-7803-7232-8.
[17] R.J.K. Wood, T.J. Harvey, G. Denuault, H.E.G. Powrie, Tribocharging, Electrostatic Sensor System characterization and Oil Chemistry Studies, Fundamental Processes of Charge Generation and Transportation in Lubricated Systems, Research (Grant Number N00014-97-1-0100), Final Technical Progress Report, Report No. ME/004, University of Southampton, School of Engineering Sciences ONR/US Navy, pp. 21–31.
[18] G. Heinicke, Tribochemistry, Akademic-Verlag, Berlin, 1984.
[19] T.J. Harvey, R.J.K. Wood, G. Denuault, H.E.G. Powrie, Investigation of electrostatic charging mechanisms in oil lubricated tribo-contacts, Tribology Int. 35 (9) (2002) 605–614.
[20] B. Sujak, A. Gieroszbski, K. Gieroszinska, Energy distribution of exoelectrons emitted into vacuum from plastically deformed, oxide covered aluminum at low temperatures, Acta Pol. A46 (1974) 1–17.
[21] A.M. James, M.P. Lord, Chemical and Physical Data, MacMillan Press Ltd., London, 1992, ISBN 0-3335-1167-0, p. 174.
[22] S. Morris, Real-time electrostatic charge monitoring of the wear surfaces and debris generated by sliding bearing steel contacts, Ph.D. thesis, 2003.
[23] H.E.G. Powrie, O.D. Tasbaz, R.J.K. Wood, C.E. Fisher, Performance of an electrostatic oil monitoring systems during an FZG gear scuffing test, in: Proceedings of the International Conference on Condition Monitoring, Swansea, 1999, Coxmore Publishing, Oxford, 1999, pp. 155–174.
[24] S.C. Lim, M.F. Ashby, Wear-mechanism maps, Acta Metall. 35 (1) (1987) 1–24.

[25] N.P. Suh, The delamination theory of wear, Wear 25 (1973) 111–124.
[26] A. Kapoor, Wear by plastic ratchetting, Wear 212 (1997) 119–130.
[27] J.F. Archard, W. Hirst, The wear of metals under unlubricated conditions, Proc. R. Soc. Lond. Ser. A, Math. Phy. Sci 236 (1206) (1956) 397–410.
[28] I.M. Hutchings, Tribology: Friction and Wear of Engineering Materials, Arnold, 1996, pp. 36–39.
[29] S. Morris, R.J.K. Wood, T.J. Harvey, H.E.G. Powrie, Electrostatic charge monitoring of unlubricated sliding wear of a bearing steel, Wear 255 (2003) 430–443.